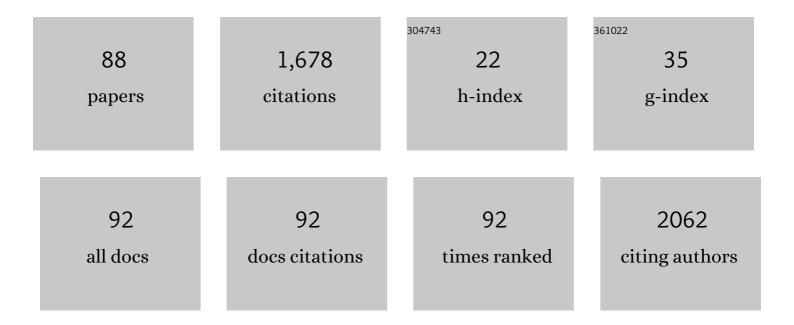
Cornelia Rodenburg

List of Publications by Year in descending order

Source: https://exaly.com/author-pdf/6984258/publications.pdf

Version: 2024-02-01



#	Article	IF	CITATIONS
1	Industrial scale manufactured superlattice hard PVD coatings. Surface Engineering, 2001, 17, 15-27.	2.2	117
2	A quantitative analysis of the influence of carbides size distributions on wear behaviour of high-speed steel in dry rolling/sliding contact. Acta Materialia, 2007, 55, 2443-2454.	7.9	96
3	High-Efficiency Spray-Coated Perovskite Solar Cells Utilizing Vacuum-Assisted Solution Processing. ACS Applied Materials & Interfaces, 2018, 10, 39428-39434.	8.0	74
4	Highâ€Performance Multilayer Encapsulation for Perovskite Photovoltaics. Advanced Energy Materials, 2018, 8, 1801234.	19.5	68
5	Quantitative secondary electron energy filtering in a scanning electron microscope and its applications. Ultramicroscopy, 2007, 107, 140-150.	1.9	56
6	Sub-nanometre resolution imaging of polymer–fullerene photovoltaic blends using energy-filtered scanning electron microscopy. Nature Communications, 2015, 6, 6928.	12.8	56
7	High resolution quantitative two-dimensional dopant mapping using energy-filtered secondary electron imaging. Journal of Applied Physics, 2006, 100, 054901.	2.5	51
8	Energy selective scanning electron microscopy to reduce the effect of contamination layers on scanning electron microscope dopant mapping. Ultramicroscopy, 2010, 110, 1185-1191.	1.9	47
9	Localized effect of Pbl ₂ excess in perovskite solarÂcells probed by high-resolution chemical–optoelectronic mapping. Journal of Materials Chemistry A, 2018, 6, 23010-23018.	10.3	47
10	The effect of residual palladium catalyst on the performance and stability of PCDTBT:PC70BM organic solar cells. Organic Electronics, 2015, 27, 266-273.	2.6	46
11	Optimizing and quantifying dopant mapping using a scanning electron microscope with a through-the-lens detector. Applied Physics Letters, 2003, 83, 293-295.	3.3	37
12	Investigation of intermixing in TiAlN/VN nanoscale multilayer coatings by energy-filtered TEM. Surface and Coatings Technology, 2002, 151-152, 209-213.	4.8	33
13	Dark electrical bias effects on moisture-induced degradation in inverted lead halide perovskite solar cells measured by using advanced chemical probes. Sustainable Energy and Fuels, 2018, 2, 905-914.	4.9	32
14	Hot workability of spray-formed AISI M3:2 high-speed steel. Materials Science & Engineering A: Structural Materials: Properties, Microstructure and Processing, 2004, 386, 420-427.	5.6	31
15	Efficient perovskite photovoltaic devices using chemically doped PCDTBT as a hole-transport material. Journal of Materials Chemistry A, 2017, 5, 15714-15723.	10.3	29
16	A comprehensive Monte Carlo calculation of dopant contrast in secondary-electron imaging. Europhysics Letters, 2008, 82, 30006.	2.0	28
17	Imaging the Bulk Nanoscale Morphology of Organic Solar Cell Blends Using Helium Ion Microscopy. Nano Letters, 2011, 11, 4275-4281.	9.1	28
18	Oxidation Behavior and Mechanisms of TiAlN/VN Coatings. Metallurgical and Materials Transactions A: Physical Metallurgy and Materials Science, 2007, 38, 2464-2478.	2.2	26

CORNELIA RODENBURG

#	Article	IF	CITATIONS
19	Quantitative secondary electron imaging for work function extraction at atomic level and layer identification of graphene. Scientific Reports, 2016, 6, 21045.	3.3	26
20	Effect of experimental parameters on doping contrast of Si p?n junctions in a FEG-SEM. Microelectronic Engineering, 2004, 73-74, 948-953.	2.4	25
21	The interface between TiAlN hard coatings and steel substrates generated by high energetic Cr+ bombardment. Surface and Coatings Technology, 2000, 125, 66-70.	4.8	24
22	Low-Voltage SEM of Natural Plant Fibers: Microstructure Properties (Surface and Cross-Section) and their Link to the Tensile Properties. Procedia Engineering, 2017, 200, 295-302.	1.2	24
23	New perspectives on nano-engineering by secondary electron spectroscopy in the helium ion and scanning electron microscope. MRS Communications, 2018, 8, 226-240.	1.8	23
24	Spinning Beta Silks Requires Both pH Activation and Extensional Stress. Advanced Functional Materials, 2021, 31, 2103295.	14.9	22
25	Site-specific dopant profiling in a scanning electron microscope using focused ion beam prepared specimens. Applied Physics Letters, 2006, 88, 212110.	3.3	21
26	Stoichiometry-dependent local instability in MAPbI ₃ perovskite materials and devices. Journal of Materials Chemistry A, 2018, 6, 23578-23586.	10.3	21
27	Shortlisted substrate ion etching in combined steered cathodic arc–ubm deposition system: effects on interface architecture, adhesion, and tool performance. Surface Engineering, 2000, 16, 176-180.	2.2	20
28	Mapping Nanostructural Variations in Silk by Secondary Electron Hyperspectral Imaging. Advanced Materials, 2017, 29, 1703510.	21.0	20
29	Mapping the potential within a nanoscale undoped GaAs region using a scanning electron microscope. Applied Physics Letters, 2004, 84, 2109-2111.	3.3	19
30	Mapping Polymer Molecular Order in the SEM with Secondary Electron Hyperspectral Imaging. Advanced Science, 2019, 6, 1801752.	11.2	19
31	Indium-free multilayer semi-transparent electrodes for polymer solar cells. Solar Energy Materials and Solar Cells, 2016, 144, 600-607.	6.2	18
32	Monitoring Carbon in Electron and Ion Beam Deposition within FIB-SEM. Materials, 2021, 14, 3034.	2.9	18
33	The Effect of Oxide Overlayers on Secondary Electron Dopant Mapping. Microscopy and Microanalysis, 2009, 15, 237-243.	0.4	17
34	Exploiting Plasma Exposed, Natural Surface Nanostructures in Ramie Fibers for Polymer Composite Applications. Materials, 2019, 12, 1631.	2.9	17
35	Mesoscale structure development reveals when a silkworm silk is spun. Nature Communications, 2021, 12, 3711.	12.8	17
36	Nanoscale Mapping of Bromide Segregation on the Cross Sections of Complex Hybrid Perovskite Photovoltaic Films Using Secondary Electron Hyperspectral Imaging in a Scanning Electron Microscope. ACS Omega, 2017, 2, 2126-2133.	3.5	16

Cornelia Rodenburg

#	Article	IF	CITATIONS
37	Understanding Surface Modifications Induced via Argon Plasma Treatment through Secondary Electron Hyperspectral Imaging. Advanced Science, 2021, 8, 2003762.	11.2	16
38	Quantitative dopant contrast in the helium ion microscope. Europhysics Letters, 2009, 86, 26005.	2.0	15
39	Searching for order in atmospheric pressure plasma jets. Plasma Physics and Controlled Fusion, 2018, 60, 014038.	2.1	15
40	Anisotropic Approach for Simulating Electron Transport in Layered Materials: Computational and Experimental Study of Highly Oriented Pyrolitic Graphite. Journal of Physical Chemistry C, 2018, 122, 10159-10166.	3.1	14
41	Making Sense of Complex Carbon and Metal/Carbon Systems by Secondary Electron Hyperspectral Imaging. Advanced Science, 2019, 6, 1900719.	11.2	14
42	Dopant contrast in the helium ion microscope. Europhysics Letters, 2009, 85, 46001.	2.0	13
43	Sub-5 nm graphene nanopore fabrication by nitrogen ion etching induced by a low-energy electron beam. Nanotechnology, 2016, 27, 195302.	2.6	13
44	Comparative study of image contrast in scanning electron microscope and helium ion microscope. Journal of Microscopy, 2017, 268, 313-320.	1.8	13
45	Controlling PbI ₂ Stoichiometry during Synthesis to Improve the Performance of Perovskite Photovoltaics. Chemistry of Materials, 2021, 33, 554-566.	6.7	13
46	Low-voltage SEM of air-sensitive powders: From sample preparation to micro/nano analysis with secondary electron hyperspectral imaging. Micron, 2022, 156, 103234.	2.2	13
47	Resolution Limits of Secondary Electron Dopant Contrast in Helium Ion and Scanning Electron Microscopy. Microscopy and Microanalysis, 2011, 17, 637-642.	0.4	12
48	Angle selective backscattered electron contrast in the low-voltage scanning electron microscope: Simulation and experiment for polymers. Ultramicroscopy, 2016, 171, 126-138.	1.9	12
49	Optimized organometal halide perovskite solar cell fabrication through control of nanoparticle crystal patterning. Journal of Materials Chemistry C, 2017, 5, 2352-2359.	5.5	12
50	Novel organic photovoltaic polymer blends: A rapid, 3-dimensional morphology analysis using backscattered electron imaging in the scanning electron microscope. Solar Energy Materials and Solar Cells, 2017, 160, 182-192.	6.2	12
51	Tensegrity Modelling and the High Toughness of Spider Dragline Silk. Nanomaterials, 2020, 10, 1510.	4.1	11
52	Solvent vapour annealing of methylammonium lead halide perovskite: what's the catch?. Journal of Materials Chemistry A, 2020, 8, 10943-10956.	10.3	11
53	High resolution dopant profiling in the SEM, image widths and surface band-bending. Journal of Physics: Conference Series, 2008, 126, 012033.	0.4	10
54	Nanoclay/Polymer Composite Powders for Use in Laser Sintering Applications: Effects of Nanoclay Plasma Treatment. Jom, 2017, 69, 2278-2285.	1.9	10

CORNELIA RODENBURG

#	Article	IF	CITATIONS
55	Optimizing size and distribution of voids in phenolic resins through the choice of catalyst types. Journal of Applied Polymer Science, 2019, 136, 48249.	2.6	10
56	Characterizing Crossâ€Linking Within Polymeric Biomaterials in the SEM by Secondary Electron Hyperspectral Imaging. Macromolecular Rapid Communications, 2020, 41, e1900484.	3.9	10
57	Identifying and mapping chemical bonding within phenolic resin using secondary electron hyperspectral imaging. Polymer Chemistry, 2021, 12, 177-182.	3.9	10
58	A novel characterisation approach to reveal the mechano–chemical effects of oxidation and dynamic distension on polypropylene surgical mesh. RSC Advances, 2021, 11, 34710-34723.	3.6	10
59	Helium ion microscopy based wall thickness and surface roughness analysis of polymer foams obtained from high internal phase emulsion. Ultramicroscopy, 2014, 139, 13-19.	1.9	9
60	"Secondary electron spectra of semi-crystalline polymers – A novel polymer characterisation tool?― Journal of Electron Spectroscopy and Related Phenomena, 2018, 222, 95-105.	1.7	9
61	Surface modification of the laser sintering standard powder polyamide 12 by plasma treatments. Plasma Processes and Polymers, 2018, 15, 1800032.	3.0	9
62	Revealing Spider Silk's 3D Nanostructure Through Low Temperature Plasma Etching and Advanced Low-Voltage SEM. Frontiers in Materials, 2019, 5, .	2.4	9
63	Hot workability of spray-formed AISI M3:2 high-speed steel. Materials Science & Engineering A: Structural Materials: Properties, Microstructure and Processing, 2004, 386, 420-427.	5.6	9
64	Arginine–glycine–aspartic acid functional branched semi-interpenetrating hydrogels. Soft Matter, 2015, 11, 7567-7578.	2.7	8
65	High-efficiency inverted polymer solar cells via dual effects of introducing the high boiling point solvent and the high conductive PEDOT:PSS layer. Organic Electronics, 2014, 15, 2059-2067.	2.6	7
66	Novel plasma treatment for preparation of laser sintered nanocomposite parts. Additive Manufacturing, 2019, 25, 297-306.	3.0	7
67	An Accurate Device for Apparent Emissivity Characterization in Controlled Atmospheric Conditions Up To 1423 K. IEEE Transactions on Instrumentation and Measurement, 2020, 69, 4210-4221.	4.7	7
68	The role of helium ion microscopy in the characterisation of complex three-dimensional nanostructures. Ultramicroscopy, 2010, 110, 1178-1184.	1.9	6
69	The effect of oxidation and carbon contamination on SEM dopant contrast. Journal of Physics: Conference Series, 2010, 241, 012078.	0.4	6
70	HelixJet: An innovative plasma source for nextâ€generation additive manufacturing (3D printing). Plasma Processes and Polymers, 2020, 17, 1900099.	3.0	6
71	A comprehensive Monte Carlo calculation of dopant contrast in secondary-electron imaging. Europhysics Letters, 2008, 82, 49901.	2.0	5
72	Dopant contrast in the Helium Ion Microscope: contrast mechanism. Journal of Physics: Conference Series, 2010, 241, 012076.	0.4	5

Cornelia Rodenburg

#	Article	IF	CITATIONS
73	Surface morphology of silica nanowires at the nanometer scale. Journal of Non-Crystalline Solids, 2011, 357, 3042-3045.	3.1	5
74	Energy filtered scanning electron microscopy: applications to characterisation of semiconductors. Journal of Physics: Conference Series, 2010, 241, 012074.	0.4	4
75	Interfacial Morphology between Ramie Fibers and Phenolic Resins: Effects of Plasma Treatment and Cure Cycle. Journal of Composite Materials, 2022, 56, 889-897.	2.4	4
76	Nanoscale Mapping of Semiâ€Crystalline Polypropylene. Physica Status Solidi C: Current Topics in Solid State Physics, 2017, 14, 1700153.	0.8	4
77	Progress towards site-specific dopant profiling in the scanning electron microscope. Journal of Physics: Conference Series, 2010, 209, 012068.	0.4	3
78	Feasibility of Plasma Treated Clay in Clay/Polymer Nanocomposites Powders for use Laser Sintering (LS). IOP Conference Series: Materials Science and Engineering, 2017, 195, 012003.	0.6	3
79	One Year On: New and Unique Applications of He Ion Microscopy. Microscopy and Microanalysis, 2009, 15, 652-653.	0.4	2
80	Energy filtered scanning electron microscopy: Applications to dopant contrast. Journal of Physics: Conference Series, 2010, 209, 012053.	0.4	2
81	Helium ion microscopy and energy selective scanning electron microscopy – two advanced microscopy techniques with complementary applications. Journal of Physics: Conference Series, 2014, 522, 012049.	0.4	2
82	Application of low-voltage backscattered electron imaging to the mapping of organic photovoltaic blend morphologies. Journal of Physics: Conference Series, 2015, 644, 012017.	0.4	2
83	Separating topographical and chemical analysis of nanostructure of polymer composite in low voltage SEM. Journal of Physics: Conference Series, 2015, 644, 012018.	0.4	2
84	Effect of experimental parameters on doping contrast of Si p?n junctions in a FEG-SEM. Microelectronic Engineering, 2004, 73-74, 948-953.	2.4	2
85	The influence of beam energy and oxidation on quantitative carbide analysis in the scanning electron microscope. Journal of Applied Physics, 2006, 100, 114902.	2.5	1
86	Energy Selective Secondary Electron Detection in SEM for the Characterization of Polymers. Microscopy and Microanalysis, 2011, 17, 880-881.	0.4	1
87	Comparison of multilayered nanowire imaging by SEM and Helium Ion Microscopy. Journal of Physics: Conference Series, 2010, 241, 012080.	0.4	0
88	Investigation of Perovskite Solar Cells Homogeneity and Defects by Complementary High-Resolution Mapping Techniques. , 0, , .		0